

# Ab initio calculation of the KRb dipole moments

S. Kotochigova, P. S. Julienne, and E. Tiesinga

*National Institute of Standards and Technology, 100 Bureau Drive, stop 8423, Gaithersburg,  
Maryland 20899.*

## Abstract

The relativistic configuration interaction valence bond method has been used to calculate permanent and transition electric dipole moments of the KRb heteronuclear molecule as a function of internuclear separation. The permanent dipole moment of the ground state  $X^1\Sigma^+$  potential is found to be  $0.30(2) ea_0$  at the equilibrium internuclear separation with excess negative charge on the potassium atom. For the  $a^3\Sigma^+$  potential the dipole moment is an order of magnitude smaller ( $1 ea_0 = 8.47835 \cdot 10^{-30}$  Cm) In addition, we calculate transition dipole moments between the two ground-state and excited-state potentials that dissociate to the K(4s)+Rb(5p) limits. Using this data we propose a way to produce singlet  $X^1\Sigma^+$  KRb molecules by a two-photon Raman process starting from an ultracold mixture of doubly spin-polarized ground state K and Rb atoms. This Raman process is only allowed due to relativistic spin-orbit couplings and the absence of gerade/ungerade selection rules in heteronuclear dimers.

PACS numbers: 03.75.Fi, 03.75.Be, 03.75.-b

In heteronuclear diatomic molecules the electrons can be distributed between the two nuclei unequally. As a result, there can be a small excess of negative charge near the more electronegative atom and thus heteronuclear dimers can have a permanent dipole moment. In this study we calculate the permanent dipole moments of the  $^1,3\Sigma^+$  electronic states of the KRb ground configuration, which dissociate to the K(4s)+Rb(5s) limit, and transition dipole moments between these states and excited states, which dissociate to K(4s)+Rb(5p) limits. Simple analysis of the ionization energies of K and Rb atoms, 4.339 eV and 4.176 eV, respectively, shows that the K atom is most likely to have an excess of a negative charge when the two atoms interact.

There are several applications of dipolar molecules in the physics of ultra-cold molecular gases. The long-range interaction between two dipolar molecules is governed by a electric dipole-dipole interaction and can, for example, significantly modify the many-body dynamics of trapped ultra-cold molecular Bose Einstein Condensates (BEC's) [1–6]. The atom-atom interactions in current atomic BEC's are spherically symmetric in origin. Following the proposal for homonuclear molecules of Ref. [7], dipolar molecules might also be formed in an optical lattice [8,9] An ultra-cold atom of each of the atomic species is held in an individual lattice site. A molecule in the electronic ground state can then be formed under the influence of laser light by inducing a two-photon transition. For any of the proposed applications, knowledge of the permanent or transition dipole moments is essential.

The dipole moments have never been determined for KRb states of the ground configuration either theoretically or experimentally. We calculate the dipole moment of the singlet  $X^1\Sigma^+$  and triplet  $a^3\Sigma^+$  states of KRb as a function of internuclear separation  $R$  using an *ab initio* configuration interaction valence bond (VB) method [10]. Both relativistic and nonrelativistic calculations are presented, which allows us to determine the influence of relativistic effects on the dipole moment. The use of configuration interaction (CI) in the VB method is essential due to the role of correlation in the formation of the molecular bond and nonzero dipole moment. The main contribution to the dipole moment of KRb is not due to the ground state atomic configuration, even though it predominantly determines the energy,

but is due to the population of excited valence and virtual orbitals.

The accuracy of the calculation of the  $X^1\Sigma^+$  wave function is tested by comparing our *ab initio* potential with existing experimental [11–14] and theoretical [15–18] singlet potentials. We also present the  $a^3\Sigma^+$  potential, compare it with the calculations of Refs. [17,18], and indicate the sensitivity of this shallow potential to the computational method.

Furthermore, we analyze the possibility of the creation of dipolar KRb molecules in an optical lattice [8]. In this Paper we calculate the transition electric dipole moments between the  $^1,^3\Sigma^+$  states of the ground configuration and relativistic  $\Omega = 0^\pm, 1$  components of excited  $^1,^3\Sigma^+$  and  $^1,^3\Pi$  states dissociating to the  $K(4s)+Rb(5p)$  limits, where  $\Omega$  is the projection of the total electronic angular momentum of the two atoms on the internuclear axis. This data provides us information about the most efficient scheme of forming KRb molecules in the singlet  $X^1\Sigma^+$  ground state from a  $K(4s)+Rb(5s)$  collision on the triplet  $a^3\Sigma^+$  potential. Moreover, we present our *ab initio* potentials for the excited states which can be used to identify the complex behavior of the transition dipole moment as function of  $R$ . Large-scale theoretical studies of the excited potentials of KRb were previously performed in Refs. [17,18]. It was shown in Refs. [19–22] that the dispersion interaction of excited KRb states is considerably stronger than in any other heteronuclear alkali dimer and that the KRb system is a good candidate for photoassociation experiments. Transition dipole moments to more-highly excited KRb states have been calculated in Ref. [17].

## I. THEORY

The electronic potentials and dipole moments are calculated with the configuration-interaction (CI) valence bond method. Both nonrelativistic and relativistic implementations of the method are used. The basic idea behind the valence-bond method is that the electronic molecular wavefunction  $|\Psi_{AB}\rangle$  is constructed from wavefunctions, which are products of wavefunctions that describe the constituent atoms  $A$  and  $B$ . In essence, the molecular wavefunction is given by

$$|\Psi_{AB}\rangle = \sum_{\alpha} C_{\alpha} |det_{\alpha}^{AB}\rangle \quad (1)$$

where each  $|det_{\alpha}^{AB}\rangle$  is an antisymmetrized ( $\hat{A}$ ) product of two atomic Slater determinants

$$|det_{\alpha}^{AB}\rangle = \hat{A}(|det_{\alpha}^A\rangle \cdot |det_{\alpha}^B\rangle). \quad (2)$$

The atomic Slater determinants  $|det_{\alpha}^A\rangle$  and  $|det_{\alpha}^B\rangle$  are constructed from one-electron functions centered on the nucleus of atom  $A$  and  $B$ , respectively. The variational CI coefficients  $C_{\alpha}$  in Eq. (1) are obtained by solving a generalized eigenvalue matrix problem, since in our approach the  $|det_{\alpha}^{AB}\rangle$  are not orthogonal.

The permanent molecular dipole moment of the molecular wavefunction  $|\Psi_{AB}\rangle$  is calculated from

$$\vec{\mu} = \sum_{k=A,B} Z_k \vec{R}_k - e \langle \Psi_{AB} | \sum_{i=1}^N \vec{r}_i | \Psi_{AB} \rangle \quad (3)$$

where  $N$  is the total number of electrons in the molecule and  $e$  is the electron charge. The first term of Eq. 3 depends on the position  $\vec{R}_k$  and charge  $Z_k$  of nuclei  $k = A$  and  $B$  and is zero by choosing an appropriate coordinate origin. The second term of Eq. 3 depends on the electronic molecular wavefunction and the electron positions  $\vec{r}_i$ . In the valence-bond method

$$\langle \Psi_{AB} | \sum_{i=1}^N \vec{r}_i | \Psi_{AB} \rangle = N \sum_{\kappa} \int d\vec{r} \vec{r} \rho^{AB}(\vec{x}, \vec{x}), \quad (4)$$

where  $\vec{x} = (\vec{r}, \kappa)$  denotes both the single-electron coordinate  $r$  and the variable  $\kappa$ . For a nonrelativistic or relativistic calculation  $\kappa$  has two or four values, respectively. The single-electron density matrix is

$$\rho^{AB}(\vec{x}, \vec{x}') = \sum_{\alpha, \beta} C_{\alpha}^* C_{\beta} \rho^{\alpha, \beta}(\vec{x}, \vec{x}'), \quad (5)$$

where the transition density matrix between determinants  $|det_{\alpha}^{AB}\rangle$  and  $|det_{\beta}^{AB}\rangle$  is defined by

$$\rho^{\alpha, \beta}(\vec{x}, \vec{x}') = (D_{\alpha\alpha} D_{\beta\beta})^{-1/2} \cdot D_{\alpha\beta} \sum_{i,j}^N (S^{-1})_{i,j}^{\alpha, \beta} \cdot \psi_i^*(\vec{x}) \cdot \varphi_j(\vec{x}'), \quad (6)$$

$D_{\alpha\beta}$  is the determinant of the  $N \times N$  overlap matrix  $S_{i,j}^{\alpha,\beta} = \langle \psi_i | \varphi_j \rangle$ , and the  $\psi_i(\vec{x}) = \langle \vec{x} | \psi_i \rangle$  and  $\varphi_i(\vec{x}) = \langle \vec{x} | \varphi_i \rangle$  denote the single-electron functions used in constructing the basis functions  $|det_{\alpha}^{AB}\rangle$  and  $|det_{\beta}^{AB}\rangle$ , respectively. Moreover,  $D_{\alpha\alpha}$  and  $D_{\beta\beta}$  are the determinants of the matrices  $S_{i,j}^{\alpha,\alpha} = \langle \psi_i | \psi_j \rangle$  and  $S_{i,j}^{\beta,\beta} = \langle \varphi_i | \varphi_j \rangle$ . The one-electron wavefunctions  $|\psi_i\rangle$  and  $|\psi_j\rangle$  are obtained by self-consistently solving Hartree-Fock and Sturmian equations for a nonrelativistic calculation and Dirac-Fock and Sturmian equations for a relativistic calculation [10]. Transition dipole moments can be derived in a similar fashion by assuming different initial and final states in Eq. 3.

## II. GROUND STATE DIPOLE MOMENTS

The atomic determinants for the KRb dimer are constructed from single-electron Hartree-Fock or Dirac-Fock functions/orbitals for electrons in closed and valence shells. Sturmian wavefunctions complement the basis functions and are used to describe virtual orbitals. One-electron functions are characterized by a main quantum number  $n = 1, 2, \dots$  and orbital angular momentum  $l = s, p, \dots$  for both nonrelativistic and relativistic calculations. In addition for relativistic calculations the one-electron orbital is labeled by the total electron spin  $j$ .

The closed shells  $1s^2 2s^2 2p^6 3s^2$  of K and  $1s^2 2s^2 2p^6 3s^2 3p^6 3d^{10} 4s^2$  of Rb form the core of the heteronuclear molecule. The superscript denotes the number of electrons in shell  $nl$ . For relativistic calculations  $2p^6$  is short for  $2p_{1/2}^2 2p_{3/2}^4$  etcetera. In our calculations excitations from these closed shells to valence and virtual orbitals are not included, i.e. all atomic determinants in the molecular basis contain the same number of electrons in these orbitals. Single electron excitations from the closed  $3p^6$  shell of K and  $4p^6$  shell of Rb are allowed and introduce core-valence correlations in the CI. The  $4s$ ,  $4p$ , and  $3d$  valence orbitals of K and  $5s$ ,  $5p$ , and  $4d$  orbitals of Rb are allowed to contain at most two electrons. In addition, for the nonrelativistic calculation we allow at most two electrons in the  $4d$ ,  $5p$ , and  $6p$  virtual orbitals of potassium and the  $5d$ ,  $6p$ , and  $7p$  virtual orbitals of rubidium. For

the relativistic calculation computational limitations restricted us to the  $4d$  and  $5p$  virtual orbitals of K and  $5d$  and  $6p$  virtual orbitals of Rb. Both covalent and ionic configurations are constructed. The CI expansions with these basis sets have 493 nonrelativistic and 1459 relativistic configurations.

The ground state potentials have equilibrium distances  $R_e$  and dissociation energies  $D_e$  that agree with experimental RKR values [13,14] and other theoretical potentials. Figure 1 shows the ground state  $X^1\Sigma^+$  and  $a^3\Sigma^+$  potentials of the KRb dimer as a function of the internuclear separation  $R$ . The solid curves of Fig. 1 describe results of our relativistic ( $\Omega = 0$ ) *ab initio* calculation whereas the dashed curves are the theoretical data of Ref. [18]. The dotted line of Fig. 1 shows the singlet RKR potential of Ref. [14].

For the  $X^1\Sigma^+$  state the difference between the two theoretical calculations shown in Fig. 1 is about 3% at  $R_e$ . A 20% difference exists at  $R_e$  of the  $a^3\Sigma^+$  potential. Our estimate of the  $C_6/R^6$  Van-der-Waals coefficient for the  $X^1\Sigma^+$  potential, obtained by fitting to the dispersion potential  $C_6/R^6 + C_8/R^8 + C_{10}/R^{10}$ , agrees to 2-3% with the value of Derevianko et. al. [23]. The experimentally determined dissociation energy for the  $X^1\Sigma^+$  potential [13,14] is  $26 \text{ cm}^{-1}$  smaller than ours.

We performed calculations of the  $X^1\Sigma^+$  and  $a^3\Sigma^+$  state potentials and their permanent dipole moments in both nonrelativistic and relativistic approximation. For the same set of one-electron orbitals the influence of relativistic effects on the potential energy is very small whereas its influence on the dipole moments is large. At  $R_e$  a relativistic calculation leads to a 30% increase in the absolute value of the dipole moment for the  $X^1\Sigma^+$  state and a 50% decrease for the  $a^3\Sigma^+$  state. Moreover, we find large correlation effects in the electric dipole moment in both nonrelativistic and relativistic calculations. The implementation of core polarization, for instance, leads a 50% of reduction in the absolute value of the dipole moment at the bottom of the singlet potential.

Figures 2 and 3 show the electric dipole moments of the  $X^1\Sigma^+$  and  $a^3\Sigma^+$  potentials of KRb as a function of internuclear separation, respectively. A negative dipole moment implies an excess electron charge on the potassium atom. The presented dipole moments

are calculated with the relativistic and nonrelativistic Hamiltonian. Curve 1 in Figs. 2 and 3 is determined from the most accurate nonrelativistic calculation, which includes the two-electron occupation of all orbitals upto  $6p$  for the K atom and  $7p$  for the Rb atom. Curve 2 in Figs. 2 and 3 shows the  $\Omega = 0$  relativistic calculation. The number of excited orbitals is smaller than in the nonrelativistic basis set and limited to excitations upto  $4d$  and  $5p$  for K atom and  $5d$  and  $6p$  for Rb atom. The difference between the dipole moments of the  $\Omega = 0$  and 1 component of the  $a^3\Sigma^+$  potential is much smaller than the uncertainties of our calculations. Tables I and II tabulate the permanent dipole moment of the  $X^1\Sigma^+$  and  $a^3\Sigma^+$  potentials shown in the figures.

Our calculation shows that the distribution of the charge density between K and Rb is very diffuse. It means that the dipole moment depends not only on the electron charge transfer from Rb to K atom but also on the induced polarization from the charge transfer, i.e. the electrons occupy excited  $p$  and  $d$  orbitals. Charge transfer and the induced polarization are of opposite sign. This is especially true for the  $a^3\Sigma$  state. We find that the excess charge is almost equal for the singlet and triplet states, but the latter has a smaller dipole moment.

The permanent dipole moments of the  $X^1\Sigma^+$  and  $a^3\Sigma^+$  state multiplied by  $R^7$ , based on a the relativistic calculation are shown in Fig. 4. It shows that the long-range behavior of the dipole moment of the two states are equal and proportional to  $1/R^7$ . This long-range behavior is due to the modification of the molecular wave function by the dipole-dipole and dipole-quadrupole multipole interactions [24].

We believe that our convergence with respect to correlation or the number of basis function is of the same order as the difference between nonrelativistic and relativistic calculation. Consequently, we feel that the most accurate dipole moment is obtained from averaging the nonrelativistic and relativistic calculation and assuming an one-standard deviation uncertainty equal to half the difference between the two calculations. For the  $X^1\Sigma^+$  state the dipole moment is  $-0.30(2) ea_0$  at  $R_e = 7.7 a_0$ , while for the  $a^3\Sigma^+$  state the dipole moment is  $-0.02(1) ea_0$  at  $R_e=11.2 a_0$ .

### III. TRANSITION DIPOLE MOMENTS

In this section we analyze the possibility of the creation of dipolar KRb molecules in an optical lattice. We assume that colliding atoms are initially in the doubly spin-polarized state, which only allow them to come together on the state  $a^3\Sigma^+$  potential. Thus photoassociation via an excited molecular  $^3\Sigma$  or  $^3\Pi$  state produces  $a^3\Sigma^+$  molecular levels. In principle this makes the production of molecules in the  $X^1\Sigma^+$  state problematical, since one has to get from the triplet to singlet spin manifold. There is, however, a viable route from the doubly spin-polarized colliding ground state atoms to ground  $X^1\Sigma$  levels via the excited state. When the detuning of the photoassociation laser from atomic resonance is small compared to the excited state spin-orbit splitting, as will be the case for most practical photoassociation schemes, then an excited  $\Omega = 0$  or 1 Hund's case (c) state can have both singlet and triplet character. Thus, an excited molecular state can be formed from excitation from a  $a^3\Sigma^+$  state that can re-emit light in a transition to a  $X^1\Sigma^+$  state. This process is absent in homonuclear dimers, since the additional gerade- ungerade selection rule for electronic transitions prevents it.

Figure 5 shows the  $\Omega = 0^\pm$  and 1 relativistic excited state potentials as a function of internuclear separation. The excited state potentials are obtained with the basis described in Sec. II. At short internuclear separation the potentials are described by the  $(^{2S+1})\Lambda^\pm$  Hund's case (a) labeling following Ref. [17] where  $\Lambda$  is a projection of the electronic orbital angular momentum on the molecular axis and  $S$  is the total electron spin. At longer  $R$  the curves are better described by  $\Omega^\pm$  Hund's case (c) labeling and relativistic effects are important. The potentials dissociate to the excited  $K(4s)+Rb(5p\ ^2P_j)$  and  $K(4p\ ^2P_j)+Rb(5s)$  fine structure limits. The two lowest dissociation limits correspond to the two fine structure states of the excited Rb atom plus a ground state K atom. The long-range behavior of the relativistic potentials dissociating to these two limits is attractive. There are seven attractive potentials with  $\Omega = 0$  and 1. Our potentials agree with the calculations of Refs. [17,18].

The attractive excited-state potentials are the most likely candidates for use in two-color



Raman photoassociation experiments. We calculate transition dipole moments relevant for transitions from the  $a^3\Sigma^+(0^-, 1)$  state, through the attractive  $\Omega = 0^\pm$  and 1 potentials, to the  $X^1\Sigma^+(0^+)$  state. Figures 6 and 7 show the nonzero transition dipole moments from the  $a^3\Sigma^+$  and  $X^1\Sigma^+$  states, respectively. Curves with the same style in the two figures indicate the same intermediate excited state. Photon selection rules ensure that  $0^+ \rightarrow 0^-$  transitions are not allowed. At long-range the transition dipole moments become independent of  $R$  and their absolute values approach the Rb  $5s \rightarrow 5p(^2P_j)$  transition dipole moment when the corresponding excited potential dissociates to the  $K(4s)+Rb(5p\ ^2P_j)$  limit.

At short-range internuclear separation the dipole moments strongly depend on  $R$ . This behavior reflects the change from a Hund's case (a) to a relativistic coupling scheme between  $20 a_0$  and  $30 a_0$ . In Fig. 6 the  $a^3\Sigma^+(\Omega = 1)$  to  $2^1\Sigma^+(0^+)$  and in Fig. 7 the  $X^1\Sigma^+(0^+)$  to  $2^3\Sigma^+(1)$  transition dipole moments approach zero at short  $R$  because singlet to triplet transitions are not allowed. In Fig. 6 both  $a^3\Sigma^+(1)$  to  $2^3\Sigma^+(1)$  and  $a^3\Sigma^+(0^-)$  to  $2^3\Sigma^+(1)$  have a small dipole moment at small internuclear separation. This can be understood by noting that the structure of the ground and excited state potentials shown in Figs. 1 and 5 is similar to that of homonuclear alkali-metal dimers, where gerade/ungerade symmetry is valid. In homonuclear dimers electric dipole transitions between gerade and ungerade states are forbidden.

The sudden change in dipole moment in Fig. 7 near  $13 a_0$  is related to the avoided crossing indicated by the circle in Fig. 5 between the  $\Omega = 1$  components of  $1^3\Pi$  and  $2^3\Sigma^+$  potentials. We estimate that the uncertainty of the transition dipole moments is  $0.1 ea_0$  based on a comparison of the calculated dipole moments at  $R = 100 a_0$  with the known  $5s$  to  $5p$  dipole moments of Rb [25].

#### IV. CONCLUSION

We determined the permanent dipole moments of the  $1,3\Sigma^+$  states of the ground configuration of the KRb heteronuclear molecule using a nonrelativistic and relativistic CI valence

bond method. The KRb permanent dipole moments are small compared to “truly” polar molecules, such as NaCl. It might, however, be large enough for experiments that aim to confine KRb in optical traps. In addition we calculated the potential energy curves and transition dipole moments to excited states correlating to K(4s)+Rb(5p) atomic limits. We have shown that there exist allowed transitions starting from colliding doubly polarized K and Rb atoms via an excited state to the singlet  $X^1\Sigma^+$  state.

The calculation of the electric dipole moments is a first step towards obtaining quantitative estimates of photoabsorption and molecular production rates in a gas of K and Rb atoms. In the future we plan to evaluate Frank-Condon factors between vibrational levels of ground and excited state potentials. In addition we need to investigate the effect of black-body radiation on the dipolar molecule by evaluating Frank-Condon factors between vibrational levels of the ground state.

## V. ACKNOWLEDGMENTS

We wish to acknowledge helpful discussions with Ilia Tupitsyn and Andrea Simoni.

## REFERENCES

- [1] S. Yi and L. You, Phys. Rev. A **61**, 041604 (2000).
- [2] K. Góral, K. Rzaszewski, and T. Pfau, Phys. Rev. A **61**, 051601 (2000).
- [3] L. Santos *et al.*, Phys. Rev. Lett. **85**, 1791 (2000).
- [4] K. Góral and L. Santos, cond-mat/0203542.
- [5] H. Pu, W. Zhang, and P. Meystre, Phys. Rev. Lett. **87**, 140405 (2001).
- [6] S. Giovanazzi, D.O'Dell, and G. Kurizki, Phys. Rev. Lett. **88**, 130402 (2002)
- [7] D. Jaksch, V. Venturi, J. I. Cirac, C. J. Williams, and P. Zoller, Phys. Rev. Lett. **89**, 040402 (2002).
- [8] B. Damski, L. Santos, E. Tiemann, M. Lewenstein, S. Kotochigova, P. Julienne, and P. Zoller, Phys. Rev. Lett. to be published, (2003).
- [9] M. G. Moore, H. R. Sadeghpour, cond-mat/0209621.
- [10] S. Kotochigova, E. Tiesinga, and I. Tupitsyn, in "New Trends in Quantum Systems in Chemistry and Physics", **1**, 219 (Kluwer Academic Publ., The Netherlands, 2001).
- [11] A. J. Ross, C. Effantin, P. Crozet, and E. Boursey, J. Phys. B **23**, L247 (1990).
- [12] N. Okada, S. Kasahara, T. Ebi, M. Baba, and H. Kato, J. Chem. Phys. **105**, 3458 (1996).
- [13] S. Kasahara, C. Fujiwara, N. Okada, H. Kato, and M. Baba, J. Chem. Phys. **111**, 8857 (1999).
- [14] C. Amiot, and J. Verges, J. Chem. Phys. **112**, 7068 (2000).
- [15] A. Yiannopoulou, T. Leininger, A. M. Lyyra, and G.-H. Jeung, Int. J. Quant. Chem. **57**, 575 (1996).

- [16] T. Leininger, H. Stoll, and G.-H. Jeung, *J. Chem. Phys.* **106**, 2541 (1997).
- [17] S. J. Park, Y. J. Choi, Y. S. Lee, and G.-H. Jeung, *Chem. Phys.* **257**, 135 (2000).
- [18] S. Rousseau, A. R. Allouche, and M. Aubert-Frecon, *J. Mol. Spectrosc.* **203**, 235 (2000).
- [19] B. Busser, Y. Ackhar, and M. Aubert-Frecon, *Chem. Phys.* **116**, 319 (1987).
- [20] S. H. Patil and K. T. Tang, *J. Chem. Phys.* **106**, 2298 (1996).
- [21] H. Wang and C. Stwalley, *J. Chem. Phys.* **108**, 5767 (1998).
- [22] M. Marinescu and H. R. Sadeghpour, *Phys. Rev. A* **59**, 390 (1990).
- [23] A. Derevianko, J. F. Babb, and A. Dalgarno, *Phys. Rev. A* **63** 052704 (2001).
- [24] D. M. Whisnant and W. Byers Brown, *Mol. Phys.* **26**, 1105 (1973).
- [25] <http://physics.nist.gov/PhysRefData/contents-atomic.html>

## TABLES

TABLE I. The electric dipole moment of the  $X^1\Sigma^+$  state. Both nonrelativistic (*nrel*) and relativistic (*rel*) results are presented. The internuclear separation  $R$  is in units of  $a_0$  and the dipole moment is in units of  $ea_0$ .

$R$	<i>nrel</i>	<i>rel</i>
6	$-2.52 \times 10^{-1}$	$-2.82 \times 10^{-1}$
6.5	$-2.60 \times 10^{-1}$	$-2.89 \times 10^{-1}$
7	$-2.69 \times 10^{-1}$	$-3.00 \times 10^{-1}$
7.5	$-2.77 \times 10^{-1}$	$-3.12 \times 10^{-1}$
8	$-2.81 \times 10^{-1}$	$-3.22 \times 10^{-1}$
8.5	$-2.80 \times 10^{-1}$	$-3.28 \times 10^{-1}$
9	$-2.72 \times 10^{-1}$	$-3.28 \times 10^{-1}$
9.5	$-2.57 \times 10^{-1}$	$-3.20 \times 10^{-1}$
10	$-2.35 \times 10^{-1}$	$-3.02 \times 10^{-1}$
11	$-1.77 \times 10^{-1}$	$-2.45 \times 10^{-1}$
12	$-1.18 \times 10^{-1}$	$-1.75 \times 10^{-1}$
13	$-7.25 \times 10^{-2}$	$-1.13 \times 10^{-1}$
14	$-4.25 \times 10^{-2}$	$-6.80 \times 10^{-2}$
15	$-2.61 \times 10^{-2}$	$-4.11 \times 10^{-2}$
16	$-1.56 \times 10^{-2}$	$-2.36 \times 10^{-2}$
18	$-6.44 \times 10^{-3}$	$-9.44 \times 10^{-3}$
20	$-2.48 \times 10^{-3}$	$-2.48 \times 10^{-3}$
22	$-1.10 \times 10^{-3}$	$-1.10 \times 10^{-3}$
24	$-5.49 \times 10^{-4}$	$-5.49 \times 10^{-4}$
26	$-3.01 \times 10^{-4}$	$-3.01 \times 10^{-4}$
28	$-1.74 \times 10^{-4}$	$-1.74 \times 10^{-4}$
30	$-1.08 \times 10^{-4}$	$-1.08 \times 10^{-4}$

32	$-6.88 \times 10^{-5}$	$-6.88 \times 10^{-5}$
34	$-4.57 \times 10^{-5}$	$-4.57 \times 10^{-5}$
36	$-3.02 \times 10^{-5}$	$-3.02 \times 10^{-5}$
38	$-2.06 \times 10^{-5}$	$-2.06 \times 10^{-5}$
40	$-1.43 \times 10^{-5}$	$-1.43 \times 10^{-5}$

---

---

TABLE II. Electric dipole moment of the  $a^3\Sigma^+$  state. Both nonrelativistic (*nrel*) and relativistic (*rel*)  $\Omega = 0$  results are presented.

$R$	nrel	rel
5	$-2.22 \times 10^{-2}$	$-1.20 \times 10^{-1}$
5.5	$-3.94 \times 10^{-3}$	$-1.13 \times 10^{-1}$
6	$1.66 \times 10^{-2}$	$-1.05 \times 10^{-1}$
6.5	$3.21 \times 10^{-2}$	$-8.21 \times 10^{-2}$
7	$3.94 \times 10^{-2}$	$-5.66 \times 10^{-2}$
7.5	$3.90 \times 10^{-2}$	$-4.54 \times 10^{-2}$
8	$3.32 \times 10^{-2}$	$-4.19 \times 10^{-2}$
8.5	$2.46 \times 10^{-2}$	$-4.05 \times 10^{-2}$
9	$1.56 \times 10^{-2}$	$-3.91 \times 10^{-2}$
9.5	$7.26 \times 10^{-3}$	$-3.71 \times 10^{-2}$
10	$4.50 \times 10^{-4}$	$-3.45 \times 10^{-2}$
10.5	$-4.67 \times 10^{-3}$	$-3.16 \times 10^{-2}$
11	$-8.18 \times 10^{-3}$	$-2.86 \times 10^{-2}$
11.5	$-1.03 \times 10^{-2}$	$-2.56 \times 10^{-2}$
12	$-1.14 \times 10^{-2}$	$-2.28 \times 10^{-2}$
12.5	$-1.17 \times 10^{-2}$	$-2.01 \times 10^{-2}$
13	$-1.13 \times 10^{-2}$	$-1.77 \times 10^{-2}$
13.5	$-1.07 \times 10^{-2}$	$-1.54 \times 10^{-2}$
14	$-9.80 \times 10^{-3}$	$-1.34 \times 10^{-2}$
14.5	$-8.82 \times 10^{-3}$	$-1.16 \times 10^{-2}$
15	$-7.83 \times 10^{-3}$	$-9.02 \times 10^{-3}$
18	$-3.24 \times 10^{-3}$	$-3.24 \times 10^{-3}$
21	$-1.22 \times 10^{-3}$	$-1.22 \times 10^{-3}$
24	$-4.78 \times 10^{-4}$	$-4.78 \times 10^{-4}$

27	$-2.04 \times 10^{-4}$	$-2.04 \times 10^{-4}$
30	$-9.67 \times 10^{-5}$	$-9.67 \times 10^{-5}$
33	$-5.18 \times 10^{-5}$	$-5.18 \times 10^{-5}$
36	$-2.72 \times 10^{-5}$	$-2.72 \times 10^{-5}$
39	$-1.54 \times 10^{-5}$	$-1.54 \times 10^{-5}$
42	$-9.14 \times 10^{-6}$	$-9.14 \times 10^{-6}$

---

---



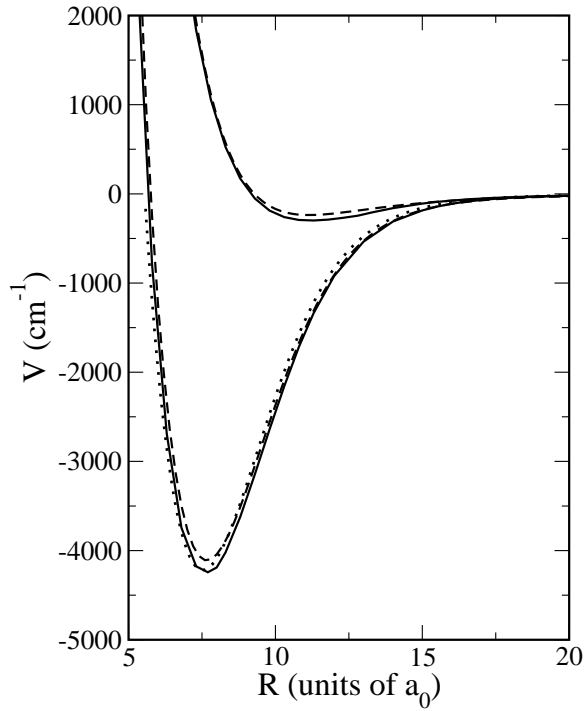


FIG. 1. The ground state  $X^1\Sigma^+$  and  $a^3\Sigma^+$  potentials of KRb as a function of internuclear separation. Solid curves are obtained in the present study, dashed lines are the results of Ref. [18], and the dotted line is the RKR potential of Ref. [14]. ( $1 a_0=0.0529$  nm)

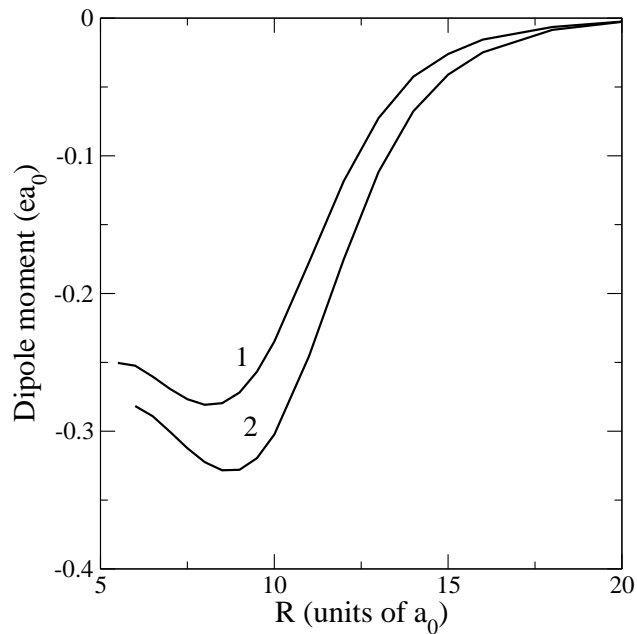


FIG. 2. The electric dipole moment of the  $X^1\Sigma^+$  ground state of the KRb dimer as a function of internuclear separation. The dipole moment is found from a nonrelativistic (curve 1) and a relativistic (curve 2) calculation.

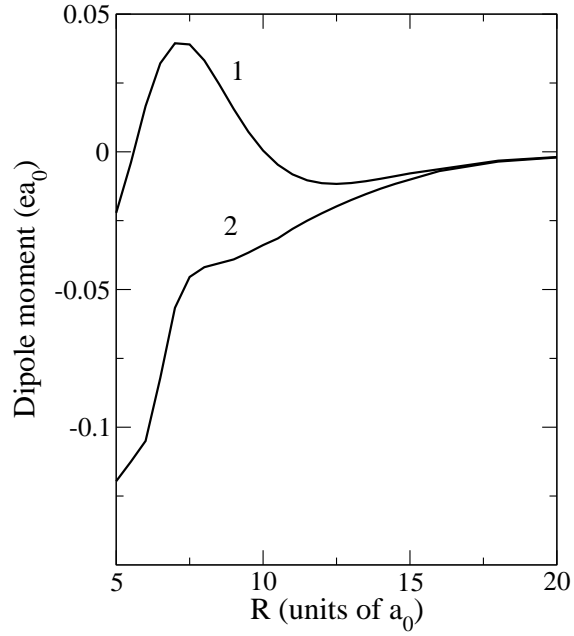


FIG. 3. The electric dipole moment of the  $a^3\Sigma^+ \Omega = 0$  state of KRb as a function of internuclear separation. The dipole moment is found from a nonrelativistic (curve 1) and relativistic (curve 2) calculation.

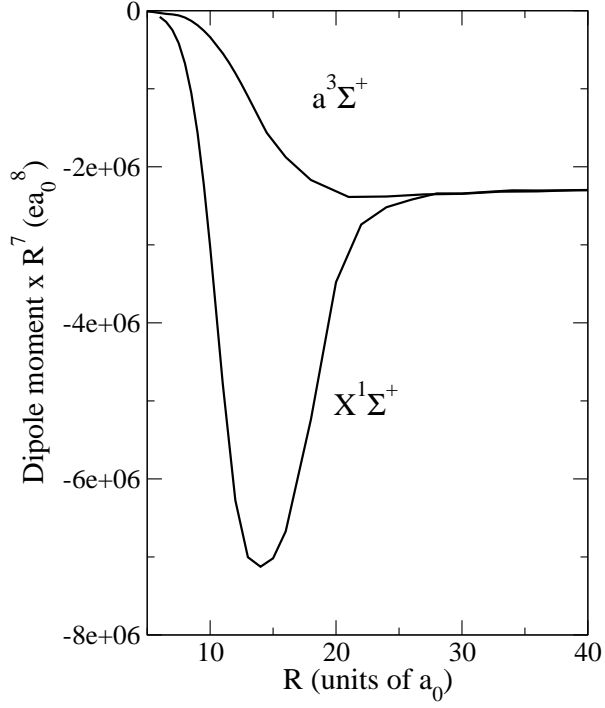


FIG. 4. The relativistic electric dipole moment multiplied by  $R^7$  of the  $X^1\Sigma^+$  and  $a^3\Sigma^+(\Omega = 0)$  states of KRb as a function of internuclear separation.

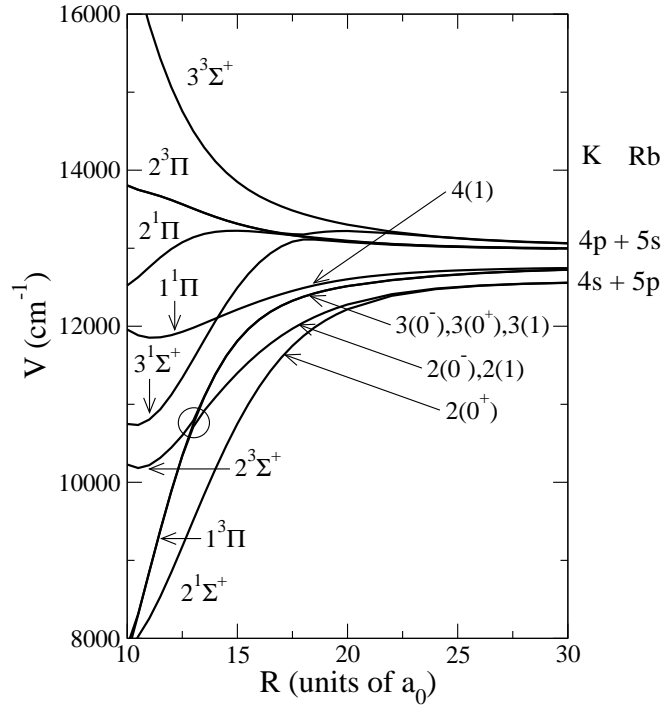


FIG. 5. Electronic  $\Omega = 0^\pm, 1$  potentials of excited states of the KRb dimer in an intermediate region of internuclear separation. The short-range  $n^{(2S+1)}\Lambda^\pm$  and long-range  $m(\Omega^\pm)$  labeling is indicated. The numbers  $n$  and  $m$  show the energy-ordered appearance of these states.

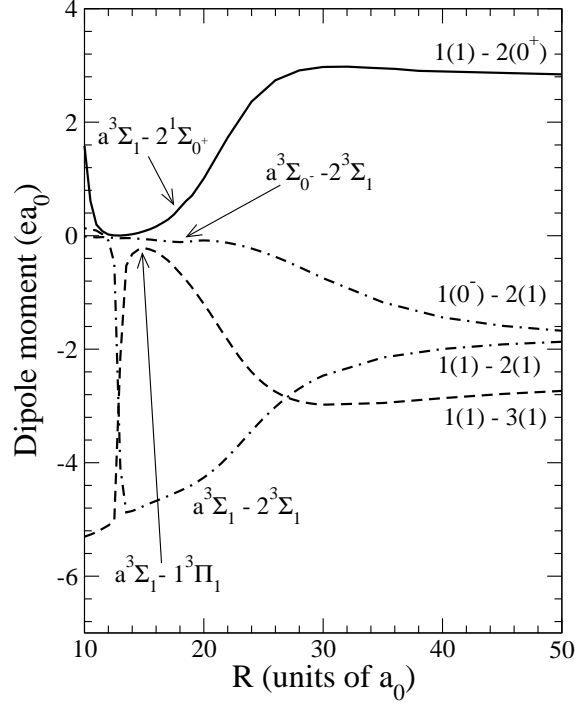


FIG. 6. Transition dipole moments between the ground  $a^3\Sigma^+$  and excited states of the KRb dimer as a function of internuclear separation. The curves are labeled by short- and long-range symmetries as in Fig. 5

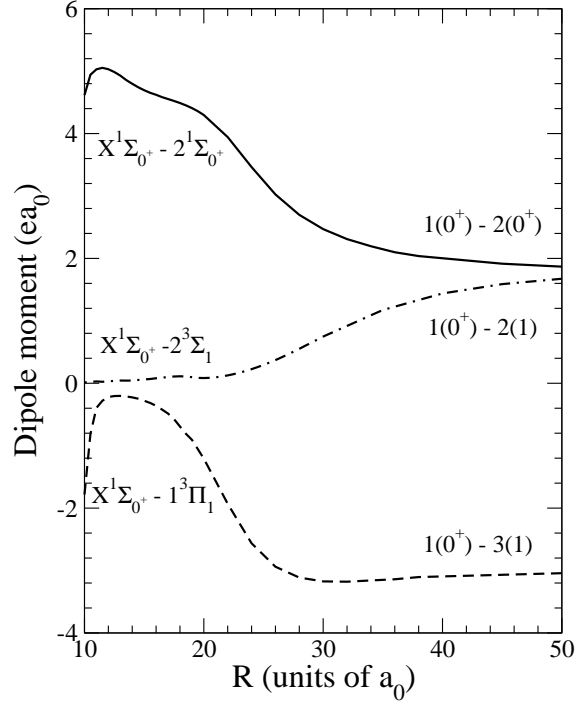


FIG. 7. Transition dipole moments between the ground  $X^1\Sigma^+$  and excited states of the KRb dimer as a function of internuclear separation. The curves are labeled by short- and long-range symmetries as in Fig. 5